NANO MICRO
small

Supporting Information

for *Small,* DOI: 10.1002/smll.202007500

Direct and Label-Free Cell Status Monitoring of Spheroids and Microcarriers Using Microfluidic Impedance Cytometry

*Lingyan Gong, Chayakorn Petchakup, Pujiang Shi, Pei Leng Tan, Lay Poh Tan, Chor Yong Tay, and Han Wei Hou**

Supplementary Information

Direct and label-free cell status monitoring of spheroids and microcarriers using microfluidic impedance cytometry

*Lingyan Gong, Chayakorn Petchakup, Pujiang Shi, Pei Leng Tan, Lay Poh Tan, Chor Yong Tay, Han Wei Hou**

Spheroid cultivation

MCF-7 (human breast cancer cell line, ATCC) was cultured in Dulbecco's Modified Eagle's Medium (DMEM, Gibco) supplemented with 10% Fetal Bovine Serum (FBS, Gibco) and 1% penicillin/streptomycin (Gibco). Upon 70% - 80% confluency, cells were harvested using 0.25% trypsin with EDTA (1 mM, Gibco). Cell suspension of specific cell densities was prepared and loaded into 0.1% pluronic acid-coated (Sigma) round bottom 96-well plate (Corning) at 100 μL per well. After centrifugation at 1300 rpm for 4 minutes, culture was maintained in humidified incubator at 37 °C and 5% CO_2 for two days for spheroid formation.

Cell Culture encapsulated in Hydrogel Microcarriers

Gelatin methacryloyl (GelMA) microcarriers were fabricated using GelMA synthesized via a one-pot method proposed by Shirahama and Lee. [1] Freeze-dried GelMA was then dissolved in phosphate buffer saline (PBS, Lonza) and added with 0.1% of cross-linker lithium phenyl-2, 4, 6-trimethylbenzoylphosphinate (LAP). HaCaT cells (immortalized human keratinocyte line) were cultured in 5% CO_2 at 37°C in regular DMEM containing glutamine supplemented

with 10% heat-inactivated FBS and 1% penicillin/streptomycin. Cell suspension of initial concentration (15×10^6 cells mL^{-1}) was mixed with GelMA pre-polymer solutions before being electrosprayed and UV cross-linked to form stable cell-laden microspheres. 3D microspheres of 460 ± 20 μm encapsulated with HaCaT cells were collected and cultured in complete DMEM media.

Cell Culture on Cytodex Microcarriers

Adipose derived mesenchymal stem cells (ADSCs) immortalized with hTERT (ATCC) were cultured in complete growth medium consisting of Mesenchymal Stem Cell Basal Medium (PCS500030, ATCC) supplemented with Mesenchymal Stem Cell Growth Kit (PCS500040, ATCC) and G418 (0.2 mg mL^{-1}). Upon 80% confluency, cells were trypsinized with 0.25% trypsin with EDTA (1 mM) and centrifuged at 300×g for 5 minutes to obtain the trypsin-free cell suspension. Dry Cytodex 3 microcarriers (Sigma) were hydrated in Ca^{2+}, Mg^{2+}-free PBS for 5 hours at room temperature. The Cytodex microcarriers (Cyto-MCs) were washed with gentle agitation for a few minutes in Ca^{2+}, Mg^{2+}-free PBS and autoclaved to sterilize. After rinsed with culture medium, microcarriers were loaded into 58 cm^2 petri dish containing 8 mL Dulbecco's Modified Eagle's Medium supplemented with 10% FBS, and 1% penicillin/streptomycin, giving a concentration of ~4×10^3 microcarriers mL^{-1}. Cell suspension with 1×10^6 cells was pipetted into the petri dish. The culture was maintained in humidified incubator at 37 °C and 5% CO_2. After 24 hours, the microcarriers were transferred to a new petri dish to remove the cells settled down and formed monolayer in petri dish. Culture was continued until 60%-80% confluency, with medium changed every two days.

Stem Cell Differentiation in Monolayer (2D)

Cell suspension of ADSCs were seeded in 6-well culture plate with complete growth medium at cell densities of 2×10^4 cells cm^{-2} and 5×10^3 cells cm^{-2} for adipogenic and osteogenic differentiation, respectively. When cells were 60% (for osteogenic differentiation) and 80% (for adipogenic differentiation) confluent, differentiation was initiated by replacing the culture medium by osteogenic medium and adipogenic medium with medium changed twice a week. Undifferentiating ADSCs were cultured in DMEM supplemented with 10% Fetal Bovine Serum (FBS, Gibco) and 1% penicillin/streptomycin (Gibco) in T75 flask, with medium changed every two days. The cultures were maintained in humidified incubator at 37 °C and 5% CO_2 for a 13-day period.

Cell viability assay

PTX-treated spheroids were washed thrice with PBS and dissociated via treatment of 0.25% trypsin with EDTA (1 mM) for 5 minutes. The harvested cells were stained with Propidium Iodide (2 μg mL^{-1}, Invitrogen) at room temperature for 15 minutes. After that, the commercial fluorescence cell counter (Arthur, NanoEntek) was used to run the cell viability assay with 25 μL stained cell suspension.

High-Speed Imaging

To capture images of spheroids/microcarriers in microfluidic channel for signal synchronization, phase-contrast videos (100 frames per second) were recorded with a Phantom V9.1 high-speed camera (Vision Research, USA) at an exposure time of 20 μs and 4× magnification.

Throughput characterization

The throughput of this device was estimated based on the impedance signal recorded at a sampling rate of 7200 data points/sec (**Figure S12**). As one spheroid flowed through the detection region, current difference between the detection and the reference electrodes yielded one peak above the baseline followed by another peak below the baseline, where the baseline indicated the impedance signal resulting from device setup. Figure S12 shows that it took less than 0.14 sec (1000 data points) for a spheroid to flow through the detection region, hence a throughput of 1 particle/sec would avoid 'multiple spheroids passing through the detection region at the same time.

Mathematical proof of membrane conductivity effects on impedance

Cell membrane can be modelled by a parallel circuit with one resistor contributing impedance independent of frequency, and one capacitor contributing frequency-dependent impedance [2]. Dead cells have higher membrane conductivity, *i.e.* $Z_R > Z_R'$. Impedance from capacitor decreases at higher frequency due to dielectric dispersion , *i.e.* $Z_C > Z_C'$. Impedance at low frequency and impedance at high frequency are denoted as *ZL* and *ZH*, respectively.

At low frequency

Membrane impedance of live cell:

$$ZL_{live} = \frac{Z_R Z_C}{Z_R + Z_C}$$

Membrane impedance of dead cell:

$$ZL_{dead} = \frac{Z_R{}' Z_C}{Z_R{}' + Z_C}$$

Difference between impedance of live and dead cells at low frequency:

$$\triangle ZL = ZL_{live} - ZL_{dead} = {Z_C}^2 \frac{Z_R - {Z_R}'}{(Z_R + Z_C)({Z_R}' + Z_C)}$$

At high frequency

Membrane impedance of live cell:

$$ZH_{live} = \frac{Z_R {Z_C}'}{Z_R + {Z_C}'}$$

Membrane impedance of dead cell:

$$ZH_{dead} = \frac{{Z_R}' {Z_C}'}{{Z_R}' + {Z_C}'}$$

Difference between impedance of live and dead cells at high frequency:

$$\triangle ZH = ZH_{live} - ZH_{dead} = {Z_C}'^2 \frac{Z_R - {Z_R}'}{(Z_R + Z_C')({Z_R}' + Z_C')}$$

Difference in effect of cell membrane conductivity on impedance at low frequency and high frequency:

$$\triangle ZL - \triangle ZH = {Z_C}^2 \frac{Z_R - {Z_R}'}{(Z_R + Z_C)({Z_R}' + Z_C)} - {Z_C}'^2 \frac{Z_R - {Z_R}'}{(Z_R + Z_C')({Z_R}' + Z_C')}$$

$$= (Z_R - {Z_R}')(Z_C - {Z_C}') \frac{(Z_R {Z_R}' + Z_R Z_C)(Z_C + Z_C') + {Z_R}' Z_C Z_C'}{(Z_R + Z_C)({Z_R}' + Z_C)(Z_R + Z_C')({Z_R}' + Z_C')}$$

$\because Z_R > {Z_R}' > 0, and\ Z_C > {Z_C}' > 0$

$\therefore$ △ZL - △ZH > 0

$\therefore$ △ZL > △ZH

$\therefore$ The effect of cell membrane conductivity on impedance at low frequency is higher than that at high frequency.

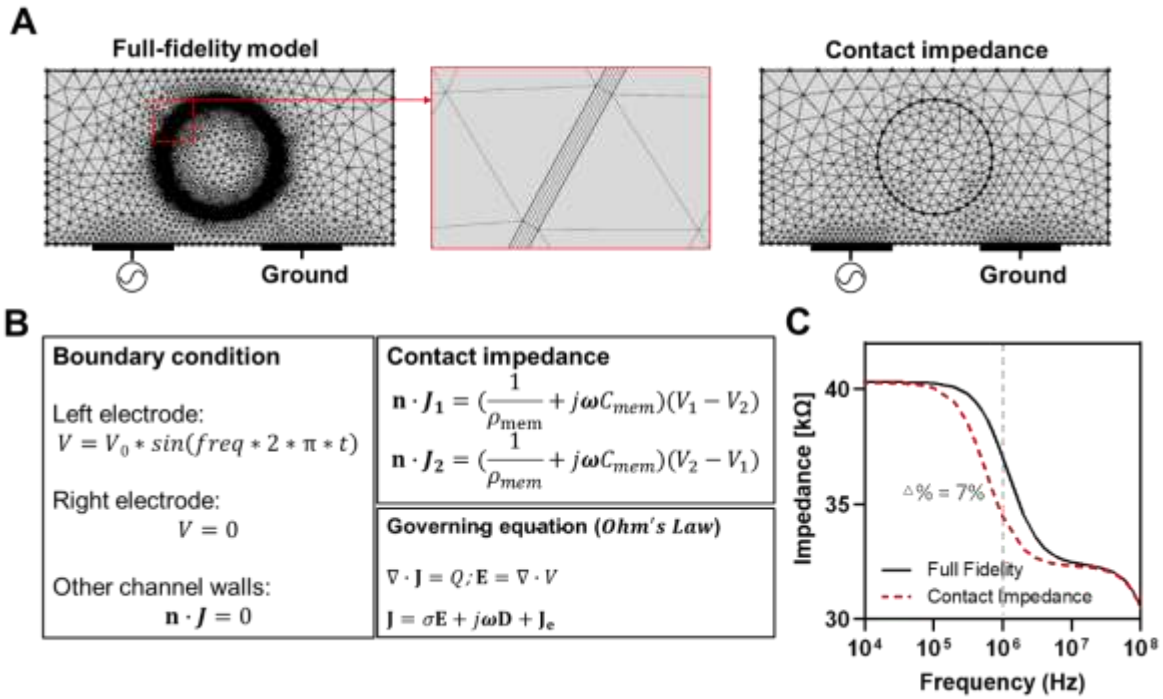

Figure S1. Comparison between full-fidelity model and contact impedance boundary condition for cell membrane modelling. (A) Numerical models that mimic a cell (circle) of radius 10 μm located at the center of a channel of height 30 μm (a section of 60 μm in length)**. (B)** Boundary conditions and governing equations of the model, where V is the electric potential, **n** is the vector normal ro the boundary, ρ_{mem} and C_{mem} are the membrane resistance and capacitance, respectively. $\mathbf{J} \equiv \mathbf{J}(x,y,t)$ is the current density (A m^{-2}), $\mathbf{E} \equiv \mathbf{E}(x,y,t)$ is the electric field (V m^{-1}), $\mathbf{D} \equiv \mathbf{D}(x,y,t)$ is the electric displacement field (C m^{-2}), $\mathbf{J_e} \equiv \mathbf{J_e}(x,y,t)$ is the external current density (A m^{-2}). **(C)** Impedance spectrums obtained from full-fidelity model and contact impedance model. The deviation mainly originated from the differences in model inputs (relative permittivity and conductivity for full-fidelity model; surface resistance and capacitance for contact impedance model) that contributed to slightly different overall membrane impedance.

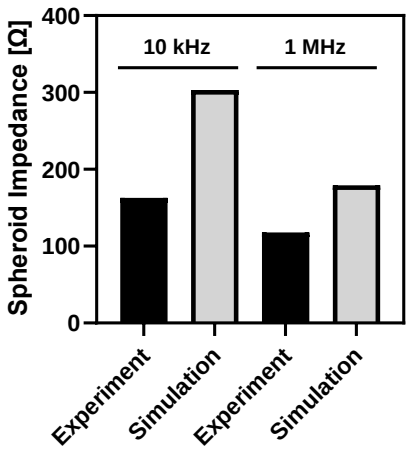

Figure S2. Comparison of spheroid impedance between experimental and simulation results. Experimental results: spheroid impedance was obtained based on the difference in impedance signals between devices with and without spheroid (measurement conducted by impedance analyzer (Palmsens4)). Simulation results: spheroid impedance was calculated based on the difference in impedance magnitudes between the channel with a 2-layer spheroid, and the channel with medium only.

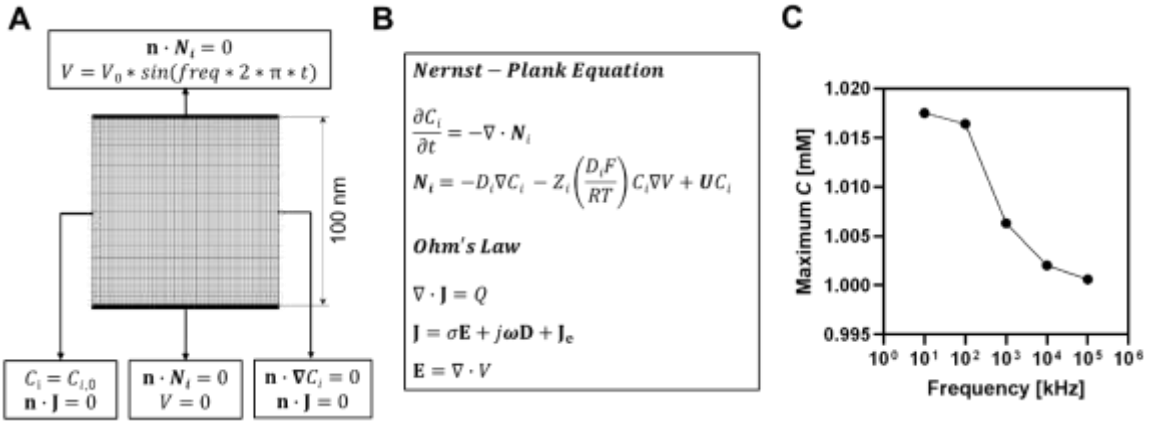

Figure S3. 2D simulation of electrical double layer. (A) Numerical model for EDL characterization labelled with boundary conditions, where $\mathbf{N}_i \equiv \mathbf{N}_i(x,y,t)$ and $C_i \equiv C_i(x,y,t)$, Z_i and D_i are the flux density (mol m^{-2} s^{-1}), ion concentration (mM), valence and the diffusion coefficient (m^2 s^{-1}) of species i (i = 1 represents cation, and i = 2 represents anion). $\mathbf{U} \equiv \mathbf{U}(x,y,t)$ is the fluid flow. V is the electric potential. V_0 = 1 mV, $C_{1,0} = C_{2,0}$ = 1 mM, , $D_1 = D_2 = 1\times10^{-9}$ m^2 s^{-1}. **(B)** Governing equations (Nernst-Plank equation and Ohm's Law) for ion transport in electric field and potential distribution, where $\mathbf{J} \equiv \mathbf{J}(x,y,t)$ is the current density (A m^{-2}), $\mathbf{E} \equiv \mathbf{E}(x,y,t)$ is the electric field (V m^{-1}), $\mathbf{D} \equiv \mathbf{D}(x,y,t)$ is the electric displacement field (C m^{-2}), $\mathbf{J_e} \equiv \mathbf{J_e}(x,y,t)$ is the external current density (A m^{-2}), and $V \equiv V(x,y,t)$ is the electric potential (V). F is Faraday's constant, R is gas constant, and T is temperature (298.15 K). The Nernst-Plank equation was coupled with ohmic conduction equation and solved in time-dependent domain to study the EDL effect. **(C)** Maximum cation concentrations in EDL at different frequencies.

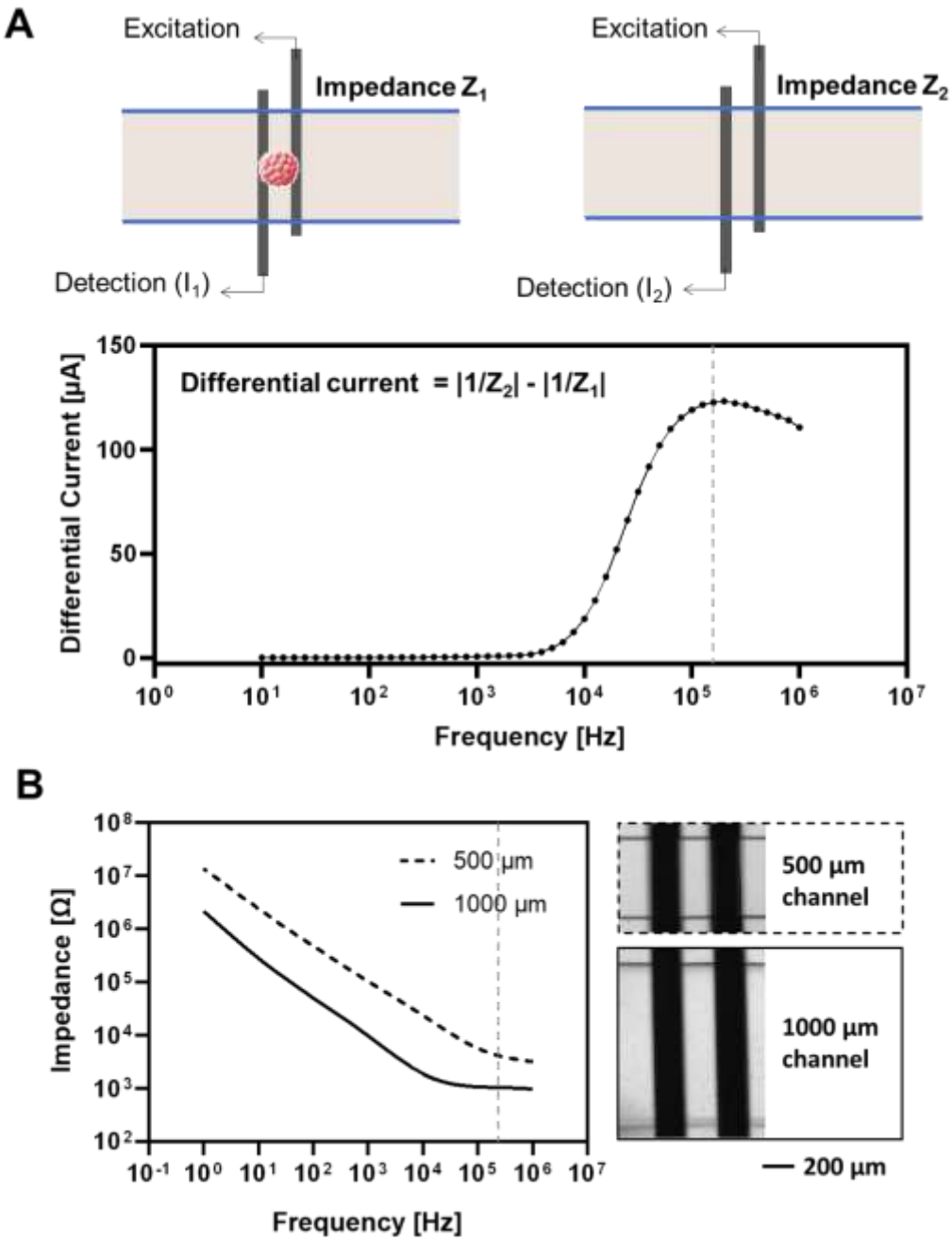

Figure S4. Impedance characterization using Palmsens4. (A) Schematic illustration of device with and without spheroid located at the center of electrodes. Differential current response indicates impedance signal of spheroid. **(B)** Impedance magnitude in 500 μm and 1000 μm channel width devices (filled with medium only). Dashed gray line at 300 kHz indicates transition of lower EDL effect.

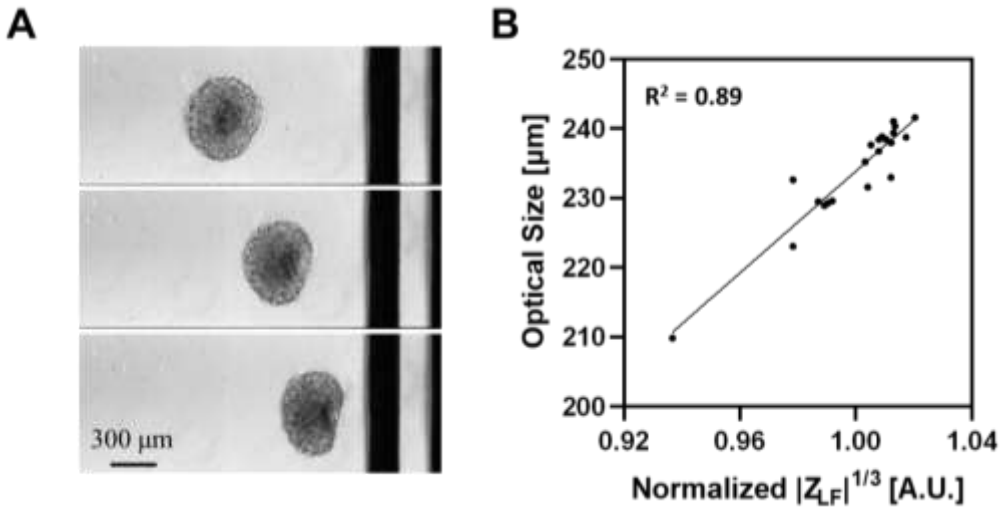

Figure S5 Correlation of particle optical size and impedance signal at low frequency $|Z_{LF}|$. (A) Representative time lapse images of a spheroid rotating as it flows through the channel. **(B)** Association between impedance signal $|Z_{LF}|$ and optical size of 250 µm polystyrene beads.

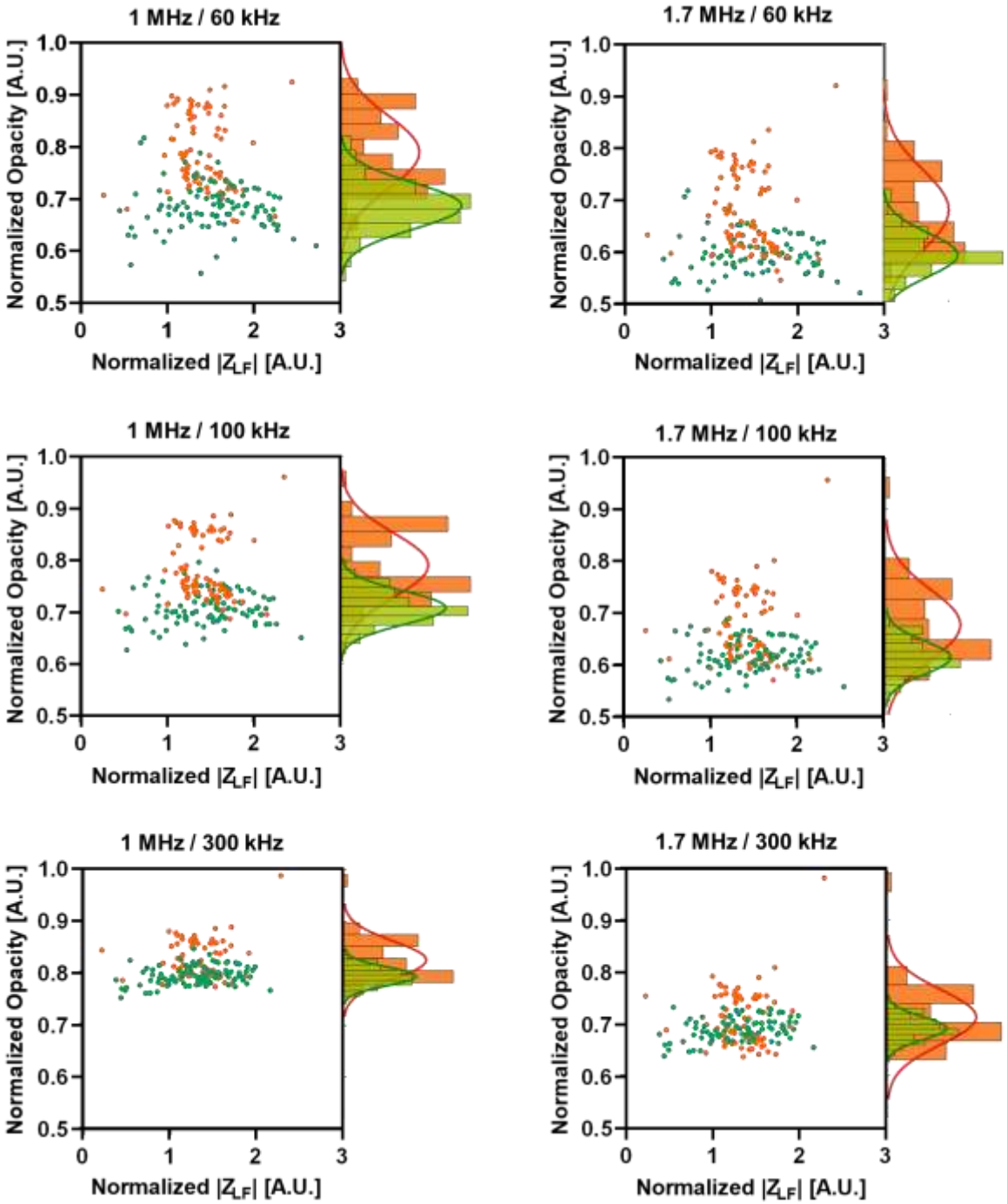

Figure S6. Frequency pair optimization. Scatter plots of impedance profile of live and dead (heat-treated) spheroids using different frequency pairs. Green: live spheroids; orange: dead spheroids.

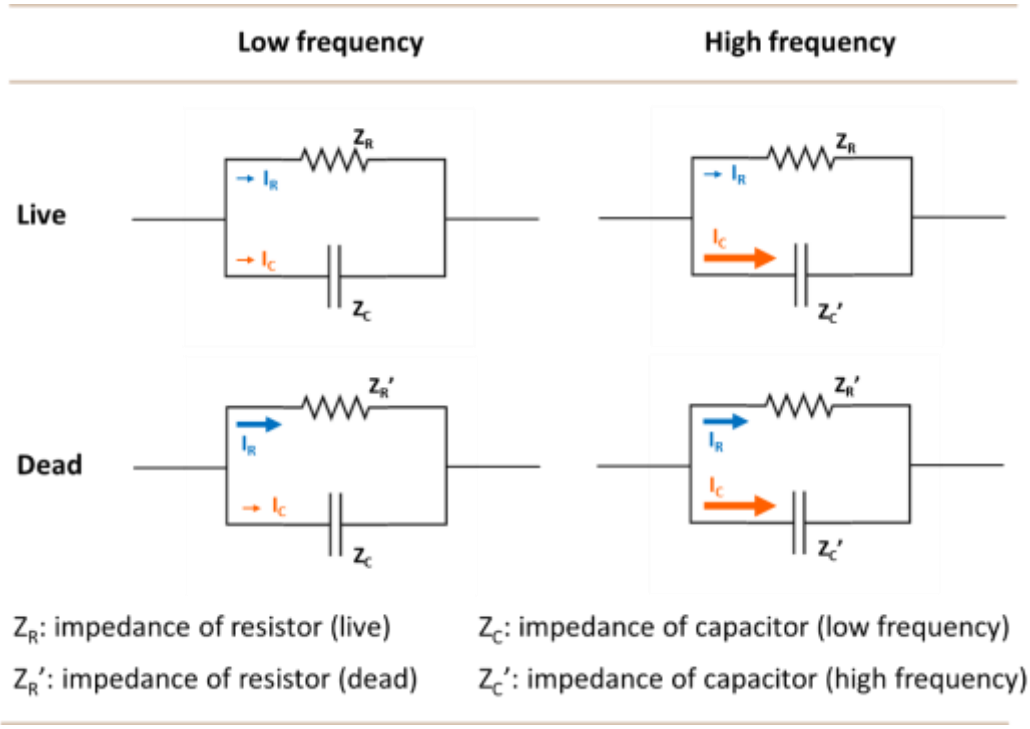

Figure S7. Equivalent circuit modelling of cell membrane using a resistor and capacitor in parallel. Larger arrows indicate higher current flow in the membrane for live and dead spheroids at different frequencies.

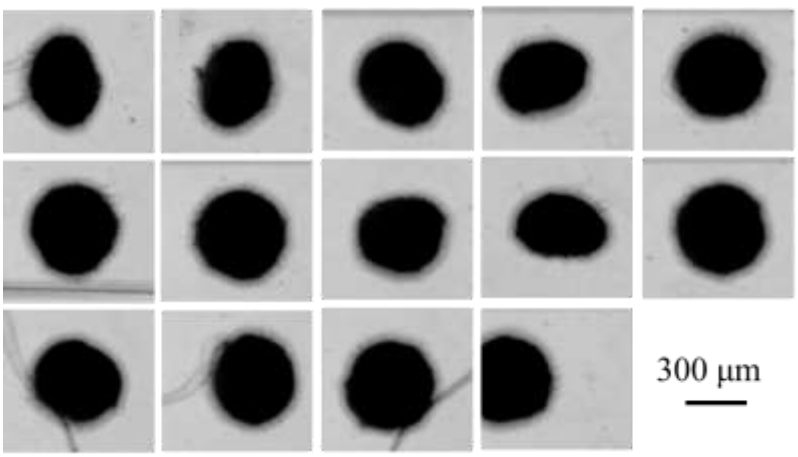

	Average deviation
$\|Z_{LF}\|$	12.73%
Opacity	3.53%
Spheroid area	4.6%

Figure S8. High-speed images of one spheroid flowing through the microchannel as it was recirculated and measured for 14 times. Scale bar is 300 µm. Black areas were quantified using ImageJ to represent the spheroid size.

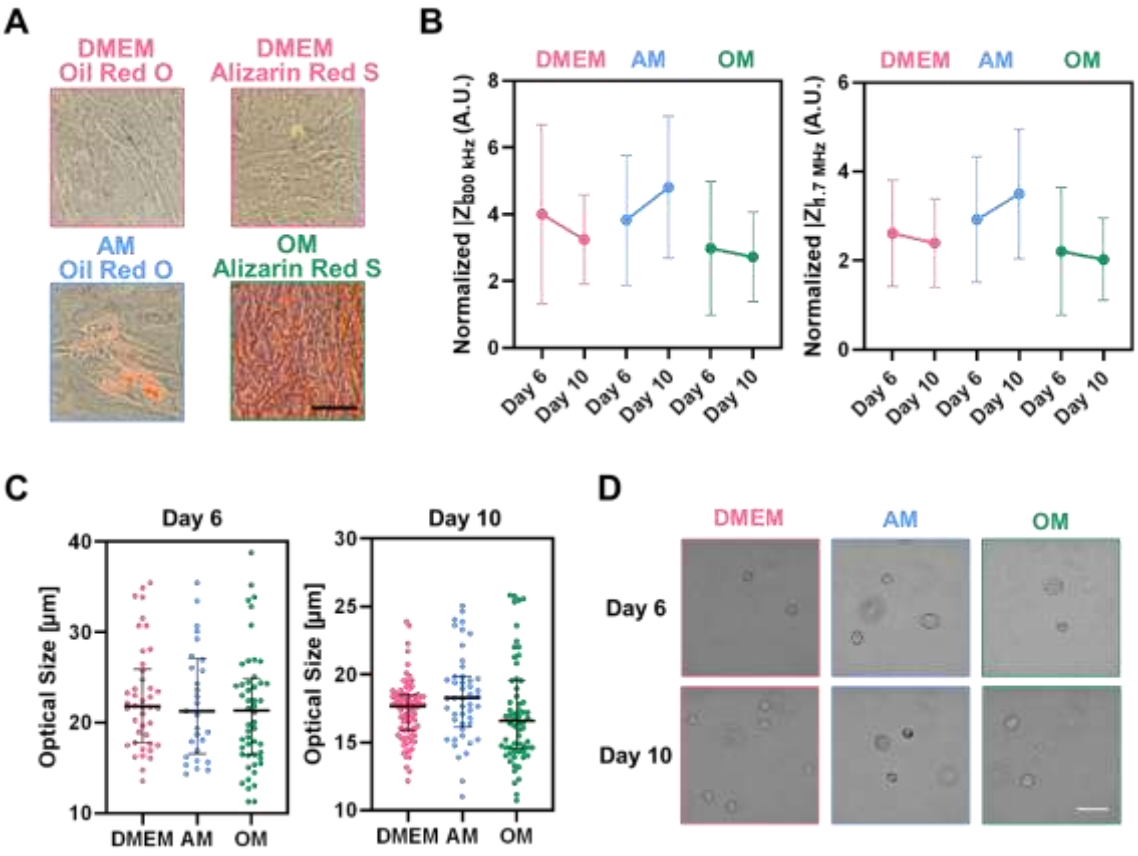

Figure S9. Single cell characterization of stem cells (ADSCs) differentiation. (A) Dye staining of differentiated ADSCs with Oil Red O and Alizarin Red S at day 10. Scale bar is 50 μm. **(B)** Normalized impedance of single differentiating cells at low (300 kHz) and high (1.7 MHz) frequencies at day 6 and day 10 of differentiation. Impedance signal of cells is normalized with 10 μm polystyrene beads. DMEM: control; AM: adipogenic cells; OM: osteogenic cells. **(C)** Optical size and **(D)** brightfield cell images at day 6 and day 10 of differentiation. Scale bar = 50 μm.

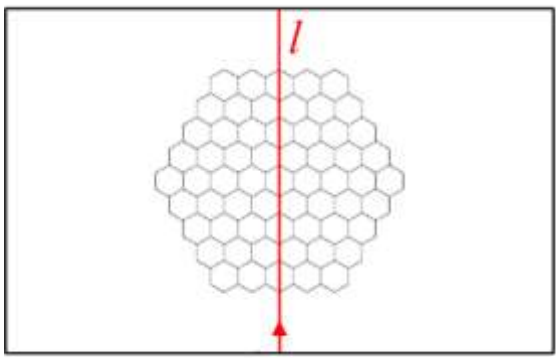

$$I = \int \boldsymbol{n} \cdot \boldsymbol{J}\, dl$$

n*: normal vector to line *l
***J*: current density**

Figure S10. Current evaluation in the 2D model.

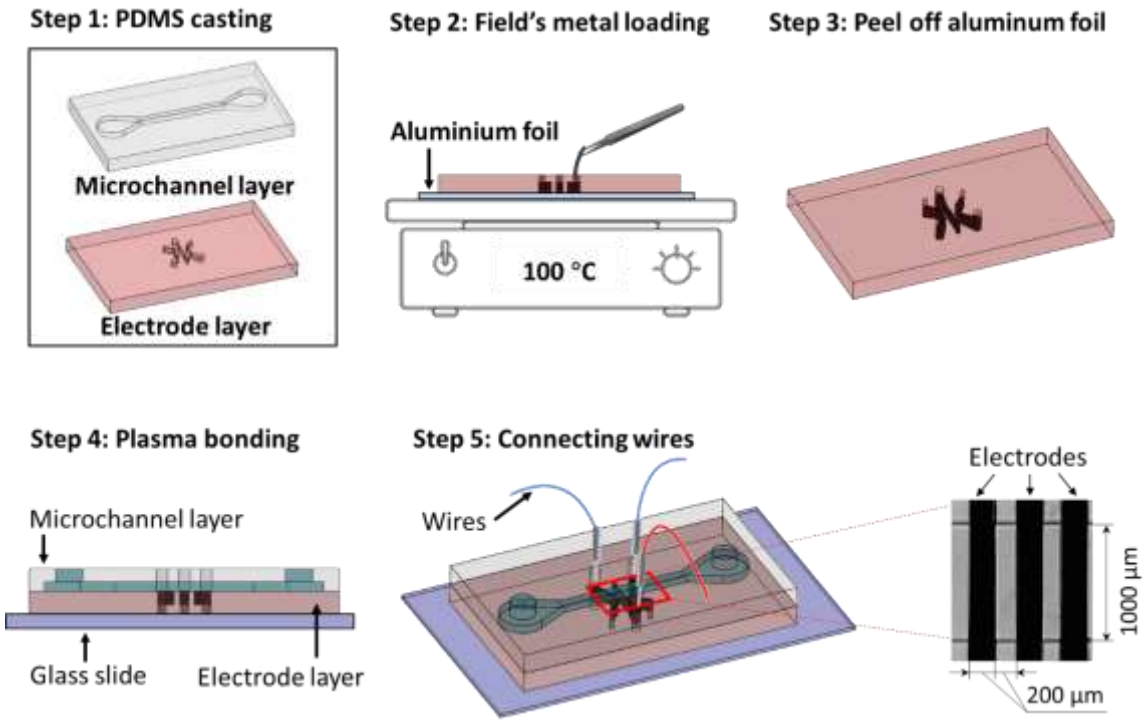

Figure S11. Overview of device design and fabrication. Step 1: PDMS device fabrication using photolithography technique. Step 2: Field's metal (melting point 62 ℃) loading into PDMS microchannels to form electrodes (bottom layer). Step 3: Peeling off an aluminium foil upon metal solidification at room temperature. Step 4: Plasma bonding of microchannel layer (gray) on top electrode layer (red). Step 5: Wire connection for electrical sensing.

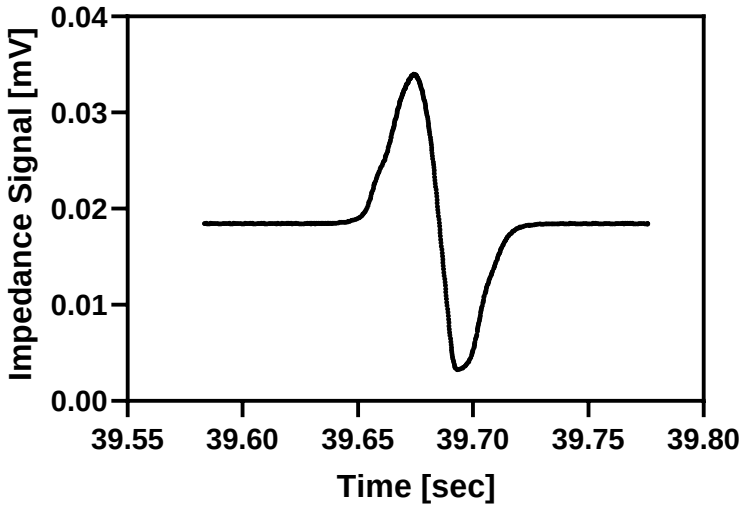

Figure S12. Impedance signal of one spheroid flowing through the detection region. Signal sampling rate is 7200 data points per second.

Table S1. Parameters for numerical simulation [3]

Parameter	Value	Parameter	Value	Parameter	Value
h	250 μm	σ_{mem}	1×10^{-7} S m^{-1}	σ_m	1.6 S m^{-1}
w	400 μm	C_{mem}	9 mF m^{-2}	ε_m	80
d_{cell}	20 μm	σ_{cyto}	0.5 S m^{-1}	σ_{gel}	0.1 S m^{-1} [4]
V_L	1	ε_{cyto}	60	ε_{gel}	80 [5]
V_R	0				

Table S2. Summary of platform applications

Applications	Key electrical signatures	Remarks
Spheroid biomass monitoring	$\|Z_{LF}\|$ [a)]	$\|Z_{LF}\|$ increases with biomass/spheroid size
Spheroid viability monitoring	Opacity [b)]	Opacity increases as cells become less viable due to the increased conductivity
Spheroid drug susceptibility monitoring	$\|Z_{LF}\|$	$\|Z_{LF}\|$ decreases at higher cytotoxicity due to the smaller spheroid size after drug treatment
Monitoring of cells encapsulated in microcarriers	Opacity, $\|Z_{LF}\|$	Opacity decreases as cells proliferate; $\|Z_{LF}\|$ increases at higher biomass
Monitoring of stem cell differentiation on Cytodex microcarriers	Opacity, $\|Z_{LF}\|$	Opacity increases as cells differentiate; $\|Z_{LF}\|$ decreases as cells differentiate into osteocytes and increases as cells differentiate into adipocytes

a) $|Z_{LF}|$: impedance at low frequency (60 kHz).

b) Opacity: ratio of impedance at high frequency ($|Z_{HF}|$, 1 MHz) to $|Z_{LF}|$

Reference

1. Shirahama, H.; Lee, B. H.; Tan, L. P.; Cho, N.-J., *Scientific Reports* **2016,** *6* (1), 31036. DOI 10.1038/srep31036.
2. Cheung, K.; Gawad, S.; Renaud, P., *Cytometry Part A* **2005,** *65A* (2), 124-132. DOI https://doi.org/10.1002/cyto.a.20141.
3. Spencer, D.; Hollis, V.; Morgan, H., *Biomicrofluidics* **2014,** *8* (6), 064124. DOI 10.1063/1.4904405.
4. Park, J.; Jeon, J.; Kim, B.; Lee, M. S.; Park, S.; Lim, J.; Yi, J.; Lee, H.; Yang, H. S.; Lee, J. Y., *Advanced Functional Materials* **2020,** *30* (39), 2003759. DOI https://doi.org/10.1002/adfm.202003759.
5. Andreas Öchsner, L. F. M. d. S., Holm Altenbach, **2018**.